academicJournals

Vol. 7(6), pp. 231-241, June, 2013
DOI :10.5897/AJPAC2013.0498
ISSN 1996 - 0840 © 2013 Academic Journals
http://www.academicjournals.org/AJPAC

African Journal of Pure and Applied Chemistry

Full Length Research Paper

Ab-initio and DFT studies of the kinetics, mechanisms and thermodynamics of the gas-phase pyrolysis of ethyl bromide

I. A. Adejoro[1], O. O. Adeboye[2]* and T. Esan[1]

[1]Department of Chemistry, University of Ibadan, Nigeria.
[2]Department of Chemistry, Emmanuel Alayande College of Education, Oyo.

Accepted 20 May, 2013

The kinetics, mechanisms, thermodynamics and vibrational studies of the pyrolysis of ethyl bromide in the gas – phase at 623 K was studied using HF at 3-21G, 6-31G* and DFT with B3LYP/6 31G*, 6-311++G (2df, 2p) basis sets. The reaction proved to be a unimolecular reaction and followed a first order rate equation. The Arrhenius parameters, such as log A with HF at 3-21G, 6-31G* = 13.93, 13.86; DFT/B3LYP at 6-31G*, 6-311++G (2df, 2p) levels = 13.61, 13.97, Ea = 228.25, 220.308 kJ/mol, ΔH = 223.25, 215.25 kJ/mol, ΔS = 14.27, 20.92 J/mol.K, ΔG = 208.99, 194.46 kJ/mol and K = 1.1 × 10^{-5}, 5.2 × 10^{-5} S^{-1} respectively are in good agreement with the experimental results.

Key words: Ab-initio, ethyl bromide, gas-phase, kinetics, mechanism.

INTRODUCTION

The presence of Cβ – H on the alkyl side of an organic halide such as hydrogen bromide, chloride and iodide gives gas–phase elimination through a four–centered cyclic transition state mechanism. Gas–phase unimolecular reactions appeared to take place through a 4-centered and 6-centered cyclic activated complex (O'Neal and Benson, 1967). Hydrogen halide elimination from the alkyl halides to produce olefins is usually four centered reactions. This reaction involves Markovnikov's addition reaction which goes through a four - centered transition states. The main aim of this study is to use ab-initio and density functional computational approach in SPARTAN to predict the kinetics, thermodynamics and the mechanism of the pyrolysis of ethyl bromide. AMI, MNDO and PM3 Hamiltonians in MOPAC with a procedure devised by (Adejoro and Emmanuel, 2010) were used to evaluate the predictive ability of these Hamiltonians to study the kinetics of the pyrolytic elimination reaction of ethyl chloride. The first order rate coefficient was calculated and was reported that the result obtained compare well with the experimental data. The kinetics and mechanism of elimination of ethyl acetate in the gas phase was also studied using PM3 semi-empirical quantum mechanical molecular orbital method. It was observed that the rate constant and the computed Arrhenius parameters compare well with the experimental values (Adejoro and Bamkole, 2009). Semi empirical PM3 and MP2/6 31G* level calculations were performed on methyl oxalyl chloride; it was observed that the mechanism implies a concerted non- synchronous process and the kinetic and thermodynamic parameters were in good agreement with the experimental method (Tania et al., 2004).

The gas-phase elimination of several ω –bromonitrile at MP2/6-31G(d,p), 6-31G(2p,2d), B1/6 31G(2d,2p) and MPW91PW91/6-31(2p,2d) levels and discovered that the

*Corresponding author. E-mail: moadeb5848@yahoo.com.

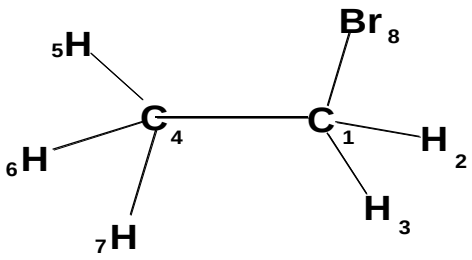

Scheme 1. The stable geometry of ethyl bromide.

calculated results were within reasonable agreement with experimental results (Jose et al., 2009). Density functional theory was used to propose the most reasonable mechanism of decomposition of 2-methoxy-1-chloroethane, 3-methoxy-1-chloropropane and 4-mehtoxy-1-chlorobutane, it was discovered that 2-methoxy-1-chloroethane, 3-methoxy-1-chloropropane proceeds through a concerted non-synchronous four-centered cyclic transition state to give olefin and 4-mehtoxy-1-chlorobutane proceeds through a five-membered transition state (Brea et al., 2012). The gas-phase elimination kinetics of several methyl $\omega -$ chloroesters using ab-initio and DFT method was studied. It was discovered that the mechanism suggest a planar concerted, non-synchronous four-membered cyclic transition state to give methyl acrylate and the calculated kinetics and thermodynamic parameters agrees well with experimental values (Romero et al., 2009).

The kinetics and mechanisms of the gas-phase elimination of 2-hydroxyphenethyl chloride and 2-methoxyphenethyl chloride appears to proceed through a three-membered cyclic transition state by the anchimetric assistance of the aromatic ring and through a free-membered cyclic transition state (Brusco et al., 2009).

COMPUTATIONAL PROCEDURE

The kinetics for the gas-phase elimination reaction of CH_3CH_2Br into HBr and C_2H_4 suggest a concerted mechanism. Conformational search was carried out on the structure using Molecular Mechanics Force Field (MMFF) which is quite successful in assigning low energy conformers and in providing quantitative estimates of conformational energy differences (Warren, 2003) to obtain the structure with the lowest energy value which is an indication of the stability of the molecule. Ethyl bromide has only one conformer and the energy is -7.717 $KJmol^{-1}$. Ab-initio and DFT methods of calculation in Spartan 10 were used for the gas-phase elimination reaction. The geometry optimization was performed on the ground state (GS), the transition state (TS) and the products to obtain the geometric parameters such as bond length, bond angle, dihedral, bond order, atomic charges and other thermodynamics parameters. H_5 is the β - hydrogen atom to be eliminated. The geometry of the ethyl bromide is defined in scheme 1:

$CH_3CH_2Br \longrightarrow C_2H_4 + HBr$

Reaction path studies

Reaction path calculations were performed on the optimized geometry of each of the alkyl vinyl ether under study using $H_5 - Br_8$ reaction coordinate. The internal coordinate was varied from its initial distance of 3.091$\dot{A}$ in the stable reactants form to its value 1.20$\dot{A}$ in the product molecule. This inter atomic distance is slowly altered throughout the reaction path calculation taking the value from 3.091 (initial value) to 1.20 Angstroms, its approximate value in the stable product molecule in 20 steps. As reported in previous work (McIver and Kormonicki 1971), instead of the energy to pass smoothly through a maximum rose to a very high value and the geometry suddenly drop to a product with a drop in the heat of formation with the values approximately the same as the sum of the expected products (hydrogen bromide and ethylene) as shown in Figure 1.

Transition state

Potential energy surfaces provide a basis for understanding the relationship between molecular structure and stability. Stable molecules correspond to energy minima along the reaction coordinate. Transition states correspond to the energy maxima. The problem is that the diagram cannot be constructed that is cannot be visualized. However, the underlying principle is that stable molecules (energy minima) will be interconnected by smooth pathway passing through well – defined transition state remain the same. The only problem is to identify this special point (stable molecules/transition state). Using the guess-transition state in Spartan on the suggested mechanism of the transition state structure was optimized and was subjected to the two tests needs to be performed in order to verify that a practical geometry corresponds to a saddle point (transition structure) and that this saddle point corresponds to the reactants and products. The tests are: That the Hessian matrix of second – energy derivations with respect to coordinates yields one and only one imaginary frequency which will be in the range of 400 to 2000 cm^{-1} and the normal coordinates corresponds to the imaginary frequency smoothly corrects reactants and products. This could be achieved by animating the normal coordinate.

The transition state was obtained by building the mechanism which follows Markovnikov's addition reaction mechanism; the transition state (TS) was confirmed by the single negative Eigen value in the Hessian matrix, intrinsic reaction coordinate and by only one imaginary IR value at absorption band 2427cm^{-1} with the intensity at 1482.95. The intrinsic reaction coordinates method was also used by optimizing the molecule subject to a fixed position along the reaction coordinate (Warren, 2003). The transition state was confirmed using the IRC method. Two IRC calculations were performed. The first one a positive perturbation was done by an initial perturbation on the atomic coordinates in the direction of the single negative frequency while the other one a negative perturbation performed along the same normal coordinates. The plot of energy in (kJ/mol) against the intrinsic reaction coordinate to ascertain the transition state is as shown in Figure 2.

Calculation

The thermodynamic calculations were obtained for ethyl bromide through calculation on the ground state GS, Transition TS and the product. The statistical mechanically calculated enthalpy and entropy was used which is not the true representative of the total energy of the molecule, knowing that the large portion of the

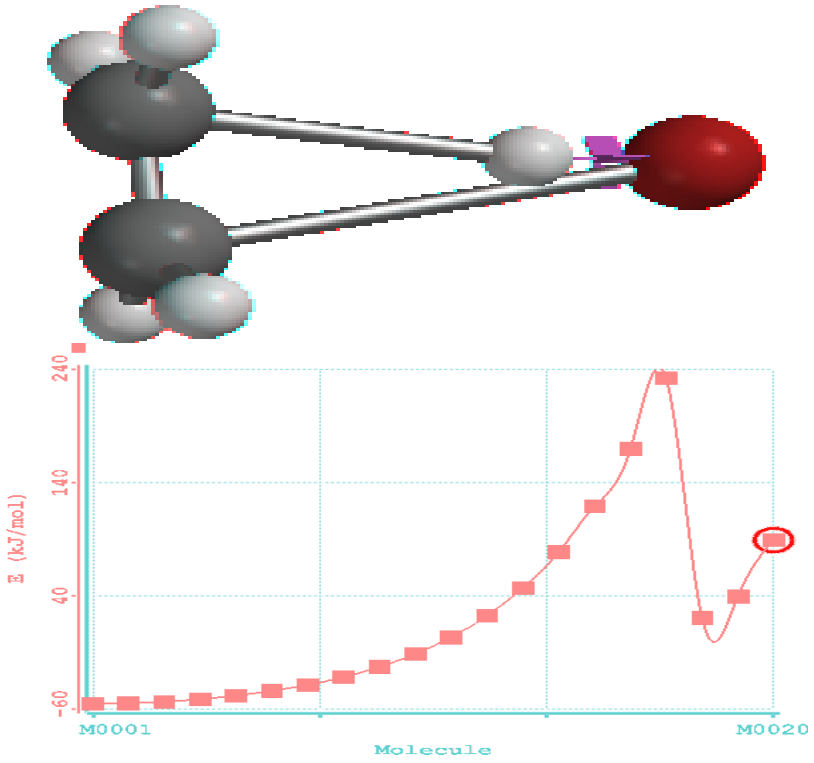

Figure 1. A plot of energy against the number of molecules to depict the reaction path studies.

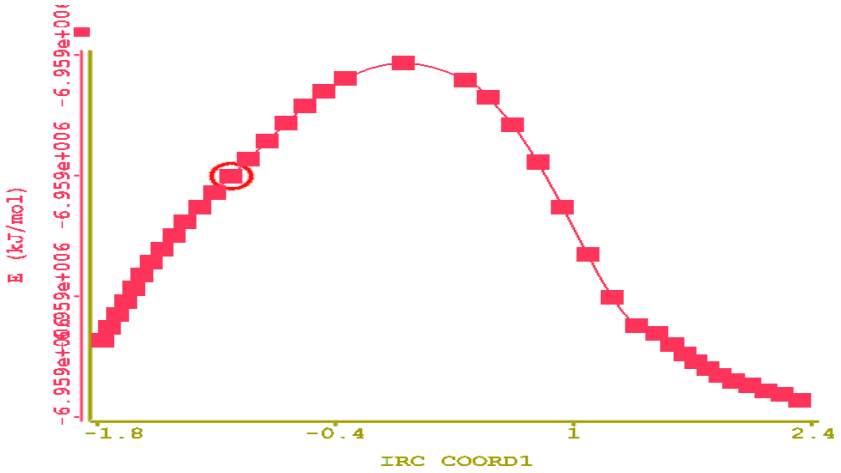

Figure 2. A plot to show the intrinsic reaction coordinate.

enthalpy in a molecule is contained in its bonds and physical conformation hence the sum of the ground state energy (GSE) and the statistical mechanically calculated enthalpy are used to arrive at a closer approximation of the true energy of the molecule. With the said modified version of the heat of reaction the equation is given as shown below (Spartan Guide to calculations). The enthalpy of a species will be defined as:

$$\mathbf{H_i} = \mathbf{GSE_i} + \mathbf{H_i}^{\mathbf{sm}} \quad (1)$$

Where, the superscript 'sm' is the statistical mechanically calculated enthalpy.

Substitute this into the initial definition of the heat of reaction, we have:

$$\Delta H_{Rxn} = \left(GSE_{product} + H^{sm}_{Product}\right) - \left(GSE_{reactant} + H^{sm}_{reactants}\right) \quad (2)$$

The enthalpy of reaction was calculated at 623 K.

Activation energy (Ea) was calculated according to the transition state theory for a unimolecular reaction at 623 K.

$$Ea = \Delta H + RT \quad (3)$$

The entropy of the reaction was calculated by taking the difference of product and reactant entropies that is:

$$\Delta S_{reaction} = S_{Product} - S_{reactants} \quad (4)$$

The Gibbs free energy was calculated using the modified version of the heat of reaction equation. Knowing that $G = H - TS$

$$\Delta G^* = \Delta H^* - T\Delta S \quad (5)$$

The first order coefficient K (T) was calculated using transition State theory (TST) (Benson, 1960) assuming that the transition coefficient is unity as shown in the following equation:

$$k(T) = \frac{K_B T}{h} \exp\left[\frac{-\Delta G^*}{RT}\right] \quad (6)$$

Where ΔG^* is the Gibbs free energy change between the reactant and the transition state and K' and h are the Boltzmann and Planck's constants respectively.

Arrhenius rate equation is given as:

$$k(T) = \frac{K_B T}{h} \exp\left[\frac{-Ea}{RT}\right] \text{ [13]} \quad (7)$$

RESULTS AND DISCUSSION

Using the HF/3 21G, HF/6 31G*, DFT/B3LYP 6-31G and 6-311++G (2df, 2p) levels, the geometry of the reactants; transition state and product were predicted as shown in Tables 1 and 2. The bond length, bond angle and dihedral were obtained and difference is about an order of magnitude for all the methods (Scheme 2).

Mechanism of decomposition of ethyl bromide

This study suggests that the gas–phase elimination reaction of ethyl bromide to give HBr and C_2H_4 occurs by a concerted non-synchronous mechanism suggesting the C_1-Br_8 as the rate- determining step. In the transition state, C_4-H_5 is stretched, HF (1.077, 1.231, 1.242, 1.252) becomes a long bond and virtually broken while the H_5–Br_8 with DFT(1.947, 2.127, 1.993, 1.979) is almost fully formed showing that the gas – phase elimination reaction of CH_3CH_2Br to give HBr and C_2H_4 proceeds through a concerted non-synchronous system which follows Markovnikov's mechanism of addition reaction (Scheme 3).

ATOMIC CHARGES

Atomic charges are shown in Mulliken. The Mulliken charges are preferred because it gives simple and reasonable estimates of atomic charges (Spartan calculation guide). The formal charges in the TS: (Table 3), show that H_5 (+0.299) has the largest charge development while Br_8 (-0.359) has the least as reported by(Ikchoon et al 1987) and the bond polarization in the C-Br, in the direction of $C^{\delta+} \cdots Br^{\delta-}$ is the rate determining step. The calculated heat of reaction of 95.0628 kJ/mol shows that the reaction needs energy to proceed. The heat of formation for the reactants, transition state and the product and reaction energetics are shown in Table 4. Kinetic calculations were done at 623 K for ab-initio and DFT methods. The calculated activation parameter that is log A as shown in Table 4 for HF/3-21G and 6-31G* levels are 13.93 and 13.86, DFT/B3LYP at 6-31G* and 6-311++G (2df, 2p) levels are 13.61 and 13.97 while the experimental values are respectively 13.5. Rates (k) for ab-initio are 4.2×10^{-5}, 2.4×10^{-5} S^{-1} and for DFT the values are 1.1×10^{-6} and 1.4×10^{-4} compared with experimental value that ranged between 1.6×10^{-6} and 2.4×10^{-5}. The activation energy (Ea) for HF (221.58 and 223.61 kJ/mol) and DFT (221.39 and 216.27 kJ/mol), change in enthalpy ΔH, HF (216.32 and 218.35 kJ/mol) and DFT (216.14 and 211.02 kJ/mol), ΔS HF (11.77 and 12.44 J/mol.K) and DFT (16.92 and 16.53 J/mol.K) and the Gibbs energy ΔG HF (200.23 and 203.92 kJ/mol) and DFT (199.22 and 194.39 kJ/mol) for ab-inito methods at 3-21G, 6-31G* levels and DFT/B3LYP at 6-31G* and 6-311++G (2df, 2p) levels respectively compares favourably well with experimental values as shown in Table 5.

The first order rate coefficient calculated within an order of magnitude compared reasonably well with the experimental value. Table 6 and the plot of temperature against rates (Figure 3) show the variation of temperature with the rate of reaction. Its shown in the table that as the temperature increases the rate of reaction also increases and rate remain constant at temperatures 573, 598 and 623 K for both AM1 and PM3; this thus validate the Arrhenius theory. Interaction between two atomic orbitals give rise to two new orbitals and one of the new orbitals has higher energy than the original (anti-bonding orbital) and the lower one (bonding orbital). The HOMO, LUMO energy characterizes the ability of electron accepting (Madhavan et al., 2011). When one of the initial orbitals is filled with a pair of electrons (a Lewis base) and the outer is empty (a Lewis acid), the two electrons can thus be placed in the lower level of the two new orbitals. This 'filled-empty' interaction has a stabilizing effect. The HOMO and LUMO (Table 7) energy for ab-initio at 3-21G and 6-31G* and DFT/B3LYP at 6-31G* HOMO- GS (-10.49, -10.78, -7.45), TS (-9.77, -8.81, N/A), PRODUCTS (-20.97, -21.99, -15.64) and LUMO GS (4.83, 4.20, -0.09), TS (-1.83, 0.67, N/A) and PRODUCTS (6.31, 8.93, 0.25) respectively reflect the HOMO as an electron donor and LUMO as an electron acceptor.

Theoretical calculations provide methods to investigate

Table 1. Bond length and bond angle.

Bond length		HF/3-21G	HF/6-31G*	DFT/B3LYP 6-31G*	DFT /B3LYP 6-31++G (2df, 2p)	Bond angle		HF/3-21G	HF/6-31G	DFT/ B3LYP 6-31G*	DFT /B3LYP 6-31++G (2df, 2p)
$C_1–H_2$	GS	1.0772	1.0777	1.0903	1.0880	$C_1–C_4–H_6$	GS	109.54	108.99	111.37	111.38
	TS	1.0706	1.0730	1.0850	1.0801		TS	111.64	111.26	118.06	118.52
	Prd	1.0737	1.0737	1.0876	1.0851		Prd	121.89	121.89	121.93	121.05
	Δq(TS-GS)	+0.005	-0.0047	-0.0053	-0.0079						
$C_1–H_3$	GS	1.0772	1.0777	1.0903	1.0850	$C_1–C_4–H_7$	GS	110.56	111.24	109.01	65.00
	TS	1.0706	1.0720	1.0860	1.0812		TS	111.64	111.26	118.07	118.55
	Prd	1.0737	1.0737	1.0876	1.0851		Prd	121.89	121.89	121.93	121.05
	Δq(TS-GS)	+0.0058	-0.0047	-0.0043	-0.0038						
$C_1–C_4$	GS	1.5294	1.5168	1.5181	1.5131	$H_2–C_1–H_3$	GS	109.94	109.38	109.31	109.40
	TS	1.3880	1.4960	1.4010	1.3922		TS	118.73	115.57	116.64	116.54
	Prd	1.3151	1.3151	1.3308	1.3361		Prd	116.21	116.21	116.13	117.90
	Δq(TS-GS)	-0.0164	-0.0208	-0.1171	-0.1209						
$C_1–Br_8$	GS	1.9631	1.9645	1.9802	1.9731	$H_2–C_1–C_4$	GS	112.05	112.28	112.42	112.54
	TS	2.8540	2.9720	2.9280	2.8500		TS	118.73	199.99	121.59	121.68
	Prd	-	-	-	-		Prd	121.89	121.89	121.93	121.05
	Δq(TS-GS)	+0.5709	+0.7105	+0.9478	+0.8769						
$C_4–H_5$	GS	1.0818	1.0828	1.0938	1.0891	$H_3–C_1–H_2$	GS	109.94	109.38	109.31	109.40
	TS	1.0770	1.2310	1.2420	1.2520		TS	115.20	115.57	116.64	116.54
	Prd	-	-	-	-		Prd	116.21	116.21	116.13	117.90
	Δq(TS-GS)	-0.0048	+0.0062	+0.1482	+0.1629						
$C_4–H_6$	GS	1.0855	1.0868	1.0981	1.0891	$H_3–C_1–C_4$	GS	112.05	122.28	112.42	112.54
	TS	1.0755	1.0760	1.0890	1.0831		TS	118.73	119.99	121.61	121.73
	Prd	1.0737	1.0737	1.0876	1.0850		Prd	121.89	121.89	121.93	121.05
	Δq(TS-GS)	-0.0135	-0.0008	-0.0091	-0.006						
$C_4–H_7$	GS	1.0818	1.0828	1.0938	1.0930	$C_4–C_1–H_2$	GS	112.05	122.28	112.42	112.54
	TS	1.0754	1.0760	1.0890	1.0832		TS	118.73	119.99	121.59	121.68
	Prd	1.0737	1.0737	1.0876	1.0851		Prd	121.89	121.89	121.93	121.05
	Δq(TS-GS)	-0.0098	+0.0032	-0.0048	-0.0098						

Table 1. Contd

H_5–Br_8	GS	3.0480	3.0790	3.1020	3.0921	C_4–C_1–H_3	GS	112.05	122.28	112.42	112.54
	TS	1.9470	2.1270	1.9930	1.9790		TS	118.73	119.99	121.61	121.73
	Prd	1.4169	1.4130	1.4335	1.4201		Prd	121.89	121.89	121.93	121.05
	Δq(TS-GS)	-0.4120	-0.2530	-1.109	-1.1131						

Table 2. Selected dihedral.

Dihedral		HF/3-21G	HF/6-31G*	DFT /B3LYP 6-31G*	DFT /B3LYP 6-31++G (2df, 2p)
H_2–C_1–C_4–H_6	GS	-62.063	61.872	-61.932	-62.09
	TS	-12.72	-16.030	-18.450	-15.79
	Prd	-0.000	-0.000	-0.000	-0.000
H_2–C_1–C_4–H_7	GS	178.146	178.682	178.674	178.49
	TS	-135.890	-139.280	-166.240	-166.82
	Prd	180.000	180.000	180.000	180.000
H_3–C_1–C_4–H_6	GS	63.063	61.872	6.932	57.33
	TS	135.950	139.240	166.130	166.99
	Prd	180.000	180.000	180.000	180.000
H_3–C_1–C_4–H_7	GS	-57.729	-57.575	-57.462	-62.09
	TS	12.780	15.990	18.350	15.97
	Prd	-0.000	-0.000	-0.000	-0.000

substantial characters of materials. The dipole moment μ for ab-initio methods at HF/ 3-21G* (2.18, 5.81 and 0.00), 6-31G* (2.51, 9.54 and 1.15), DFT/B3LYP 6-31G* (2.32, 6.18 and 1.11) and DFT/B3LYP/6-311++G*(2df, 2p) level (2.15, 6.02 and 0.00) at the ground state, transition state and products shows as shown in Table 8. The IR values obtained theoretically as shown in Table 9 compares favourably well with experimental values for instance the $\upsilon(C\text{-}H)_{str\ sp^2}$ (3036 to 3101cm^{-1}), $\upsilon(C\text{-}H)_{str\ sp^3}$ (3051 to 3153 cm^{-1}), obtained theoretically against experimental results $\upsilon(C\text{-}H)_{str\ sp^2}$ (3100 to 3010 cm^{-1}) for the reactant and for the products $\upsilon(C{=}C)_{str}$ (1827 cm^{-1}), $\upsilon(C\text{-}H)_{str\ sp^2}$ (3153 to 3217 cm^{-1}) and $\upsilon(H\text{-}Br)_{str}$ (2439 cm^{-1}) against experimental values of $\upsilon(C{=}C)_{str}$ (1680 to 1620 cm^{-1}), $\upsilon(C\text{-}H)_{str\ sp^2}$ (3100 to 3010 cm^{-1}) with the corresponding IR spectra as shown in Figure 4.

Conclusion

In conclusion, all the results are consistent with theexperimental result. The result shows that the reaction proceeds in a concerted non-synchronous four centered mechanism which

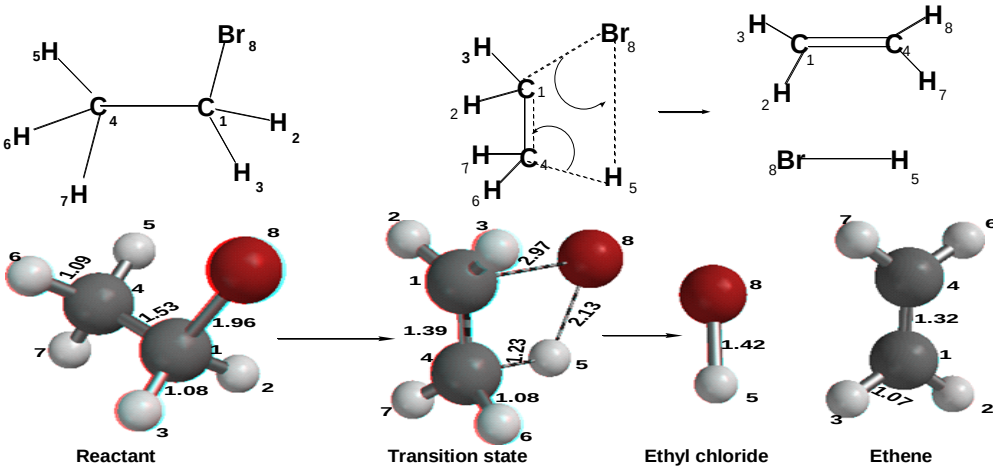

Scheme 2. Reaction with the corresponding bond length at the ground state, transition state and products.

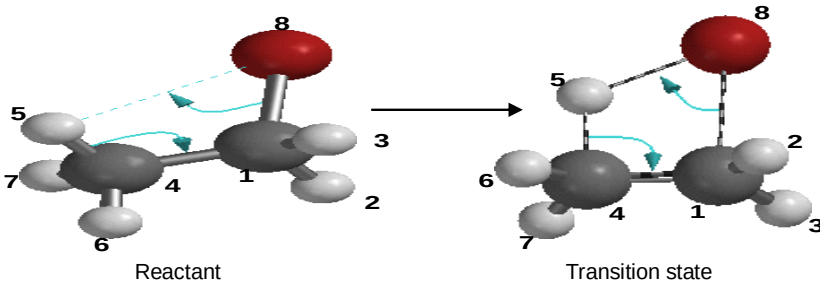

Scheme 3. Reaction mechanism.

Table 3. Atomic charges (Mulliken).

Atoms		HF/3-21G	HF/6-31G*	DFT/B3LYP 6-31G*	DFT /B3LYP 6-31++G (2df, 2p)
C_1	GS	-0.457	-0.0365	-0.324	-0.366
	TS	-0.170	-0.154	-0.156	-0.308
	Prd	-0.285	-0.353	-0.285	-0.209
	Δq(TS-GS)	+0.287	+0.211	+0.168	+0.058
H_2	GS	+0.255	+0.215	+0.193	+0.119
	TS	+0.316	+0.303	+0.234	+0..300
	Prd	+0.143	+0.176	+0.143	+0.105
	Δq(TS-GS)	+0.061	+0.088	+0.041	+0.181
H_3	GS	+0.255	+0.255	+0.193	+0.119
	TS	+0.316	+0.316	+0.234	+0.138
	Prd	+0.143	+0.143	+0.143	+0.105
	Δq(TS-GS)	+0.061	+0.061	+0.041	+0.019
C_4	GS	-0.603	-0.488	-0.443	+0.048
	TS	-0.776	-0.549	-0.485	-0.049
	Prd	-0.285	-0.353	-0.285	-0.213
	Δq(TS-GS)	-0.173	-0.061	-0.042	-0.097

Table 3. Contd

H_5	GS	+0.228	+0.190	+0.173	+0.112
	TS	+0.370	+0.301	+0.236	+0.138
	Prd	+0.225	+0.l94	+0.188	-0.209
	Δq(TS-GS)	+0.142	+0.111	+0.063	+0.026
H_6	GS	+0.212	+0.174	+0.157	+0.099
	TS	+0.282	+0.267	+0.210	+0.180
	Prd	+0.143	+0.176	+0.143	+0.105
	Δq(TS-GS)	+0.070	+0.093	+0.053	+0.081
H_7	GS	+0.228	+0.190	+0.173	+0.112
	TS	+0.282	+0.266	+0.210	+0.181
	Prd	+0.143	+0.176	+0.143	+0.105
	Δq(TS-GS)	+0.054	+0.036	+0.037	+0.069
Br_8	GS	-0.119	-0.131	-0.122	-0.243
	TS	-0.621	-0.787	-0.484	-0.580
	Prd	-0.225	-0.194	-0.188	+0.213
	Δq(TS-GS)	-0.502	-0.656	-0.362	-0.337

Table 4. Heat of formation of reactants (GS), transition (TS) and product and reaction energetics (kJ/mol).

	GS	TS	Products	$\Delta E^{*}(E_T - E_R)$	$\Delta E^{U} = E_P - E_R$
HF/3-21G	-6926024.17	-6925715.74	-6925914.45	308.44	109.72
HF/6-31G*	-6958232.92	-6957963.34	-6956998.65	269.59	1234.28
DFT/B3LYP/631G*	-6964419	-6964184.43	-6964306.23	234.57	112.77
DFT/B3LYP 6-311++G (2df, 2p)	-6965269.56	-6965042.98	-6965184.20	226.58	84.8

Table 5. Activation parameters at 623 K.

	Ea (kJ/mol)	ΔH(kJ//mol)	ΔS(J/molk)	ΔG(kJ/mol)	Log A	K (S^{-1})	Ref
HF/3-21G	221.58	216.32	11.77	200.23	13.93	4.2×10^{-5}	
HF/6-31G*	223.61	218.35	14.44	203.92	13.86	2.4×10^{-5}	
DFT/B3LYP/6-31G*	221.39	216.14	16.92	199.22	13.61	1.1×10^{-5}	
DFT/B3LYP/6-311++G*(2df, 2p)	216.27	211.02	16.53	194.49	13.97	1.3×10^{-4}	
Experimental calculated	225.67	220.61	N/A	N/A	13.50	1.6×10^{-6}	1 and 4
					12.86	8.8×10^{-7}	
					13.45	3.4×10^{-7}	
					12.95	1.0×10^{-6}	
					12.85	8.6×10^{-7}	
					13.30	2.4×10^{-6}	

follows Markovnikov reaction mechanism because the transition state look more product-like or late with respect to the reaction progress is in agreement with Brea (2012). The activation parameters and the first order rate coefficient as shown in Table 5 are within an order of magnitude and agree perfectly well with the experimental value. As discovered by (Adejoro and Emmanuel 2010) for ethyl chloride in the predictive ability of three

Table 6. Variation of rate of reaction with temperature.

Temperature (K)	Rate (ˉS) AMI	Rate (ˉS) PM3
448	3.8×10^{-5}	8.6×10^{-6}
478	4.2×10^{-5}	8.9×10^{-6}
498	4.4×10^{-5}	9.6×10^{-6}
523	4.5×10^{-5}	9.7×10^{-6}
548	5.0×10^{-5}	1.0×10^{-5}
573	5.2×10^{-5}	1.1×10^{-5}
598	5.2×10^{-5}	1.1×10^{-5}
623	5.2×10^{-5}	1.1×10^{-5}

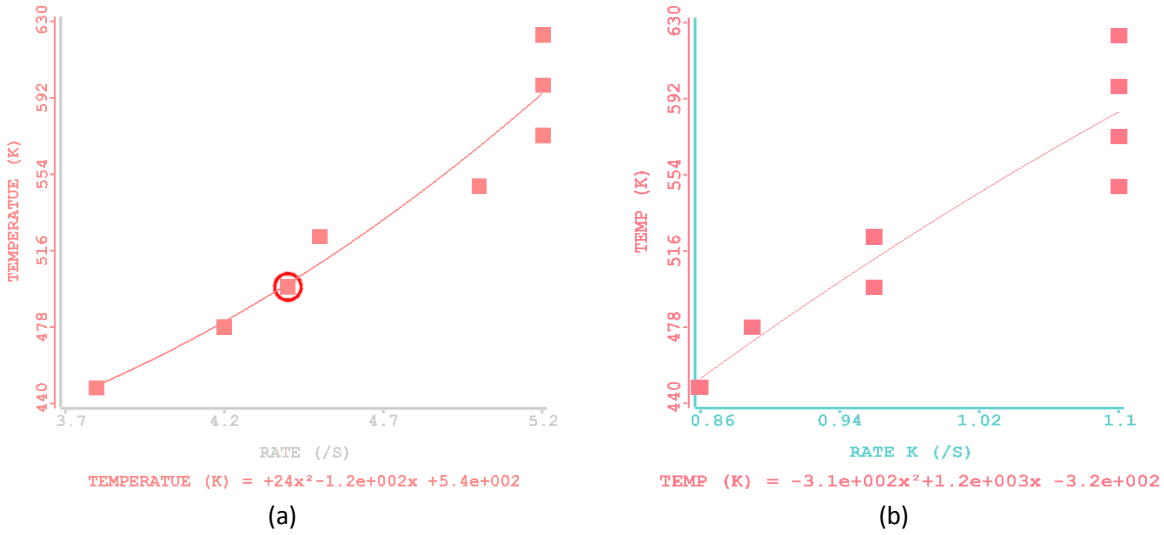

Figure 3. Plot of temprature/rate (AM1) (a) and plot of temprature/rate (PM3) (b).

Table 7. Highest occupied molecular orbital and lowest unoccupied molecular orbitals (E-HOMO and E-LUMO) (eV).

		HF/3-21G	HF/6-3 1G	DFT/B3LYP/6 31G	DFT/B3LYP/6-311++G*(2df, 2p)
E- HOMO	GS	-10.49	-10.78	-7.45	-7.61
	TS	-9.77	-8.81	-6.39	-6.61
	PRODUCT	-20.97	-21.99	-15.64	-16.21
E-LUMO	GS	4.83	4.20	-0.09	-0.59
	TS	-1.83	0.67	-3.68	-3.67
	PRODUCT	6.31	8.93	0.25	-1.21

Table 8. Dipole moment (debye).

	GS	TS	PRODUCT
HF/3 21G	2.18	5.81	0.00
HF/6 31G*	2.51	9.54	1.15
DFT/B3LYP 6-31G*	2.32	6.18	1.11
DFT/B3LYP/6-311++G*(2df, 2p)	2.15	6.02	0.00

Table 9. Infra red (CM^{-1}).

	Experimental	Calculated
Reactant		
$\upsilon(C\text{-}H)_{bend}$	N/A	1052 - 1435
$\upsilon(C\text{-}H)_{str\ sp^2}$	3100 - 3010	3036 - 3101
$\upsilon(C\text{-}H)_{str\ sp^3}$	2950 - 2850	3051 - 3153
Product1 (ethene)		
$\upsilon(C\text{-}H)_{bend}$	N/A	1056 - 1413
$\upsilon(C{=}C)_{str}$	1680 - 1620	1827
$\upsilon(C\text{-}H)_{str\ sp^2}$	3100 - 3010	3153 - 3217
Product 2 (HBr)		
$\upsilon(H\text{-}Br)_{str}$	N/A	2439

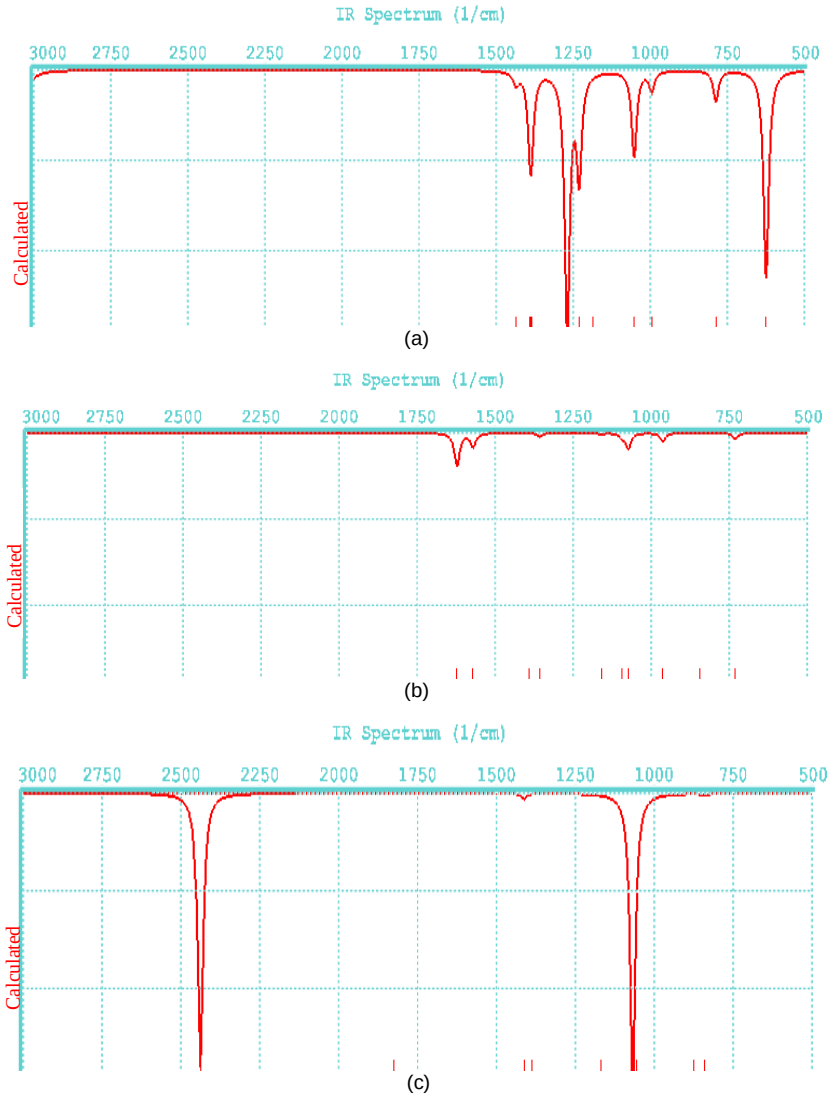

Figure 4. IR spectra of the reactant (GS) (a), transition state (TS) (b) and products (c).

Hamiltonians (AM1, PM3 and MNDO) in MOPAC, AM1 also compares favourably well with experimental values in ethyl bromide.

REFERENCES

Adejoro IA, Bamkole OT (2009). Kinetics and Mechanism of elimination of ethyl acetate in the gas phase: A theoretical study. Afr. J. Pure Appl. Chem. 3:7.

Adejoro IA, Emmanuel E (2010). Theoretical Study of the Kinetics of the Pyrolytic Elimination Reaction of Ethyl Chloride. E- J. Chem. 7(1):271- 274.

Brea O, Loroño M, Marquez E, Mora JR, Cordova T, Chuchani G (2012). Theoretical study of methoxy group influence in the gas-phase elimination kinetics of methoxyalkyl chlorides. Int. J. Quantum Chem. 112: 2504–2514

Brusco Y, Berroteran N, Loroño M, Córdova T, Chuchani G (2009). Theoretical calculations for neighboring group participation in gas-phase elimination kinetics of 2-hydroxyphenethyl chloride and 2-methoxyphenethyl chloride. J. Phys. Org. Chem. 22:1022-1029

Ikchoon L, Young S, Park YS, Bon-Su L (1987). Determination of reactivity by MO Theory (Part 50). MO studies on the Gas Phase Pyrolysis of Ethers, Bull, Korean Chem. Soc. 8(3):193-196.

IR Absorption Table. www.chem.ucla.edu/~webspectra/irtable.html.

Jose RR, Marcos L, Jose R, Mora R, Dominguez M, Tania C, Gabriel C (2009). Theoretical studies of the gas-phase pyrolysis kinetics of -bromonitriles, ZCH2CH2Br [Z=NC, NCCNH2, NCCH2CH2, Int. J. Chem. Kinet. 41:168-175.

Madhavan J, Arulmozhi S, Victor AR (2011). HOMO, LUMO analysis and first order hyperpolarizability of 2-amino-5-chlorobenzophenone using computational methods. Pelagia Research Library Der Chemica 2(6):158-163.

McIver Jr JW, Kormonicki A (1971). Rapid Geometry Optimization for Semi- Empirical Molecular Orbital Methods. Chem. Phys. Lett. 10:303.

O'Neal HE, Benson SWA (1967). Method for estimating the Arrhenius A factor for four and Six – Center Unimolecular Reactions. J. Phys. Chem. 71(9):2911.

Romero ML, Cordova T, Chuchani G (2009). Theoretical study of neighboring group participation of methyl ω-chloroesters elimination kinetics in the gas phase. J. Phys. Org. Chem. 22:403-409

Spartan Calculation Guide. www.engin.umich.edu/~cre/web_mod/quantum/topic03.htm

Tania C, Alexandra R, Gabriel C (2004). Experimental and theoretical study of the homogenous, unimolecular gas-phase elimination kinetics of methyl oxalyl chloride. J. Phys. Org. Chem. Wiley InterScience (www.interscience.wiley.com). 17:148-151.

Warren JH (2003). A Guide to molecular Mechanics and Quantum Chemical Calculations. Irvine USA. P.399.